Received 10 August 2018
Revised 30 November 2018
Accepted 31 January 2019

Fractional order super-twisting sliding mode observer for sensorless control of induction motor

Erdem Ilten and Metin Demirtas
Department of Electrical and Electronics Engineering, Balikesir University, Balikesir, Turkey

Abstract

Purpose – To meet the need of reducing the cost of industrial systems, sensorless control applications on electrical machines are increasing day by day. This paper aims to improve the performance of the sensorless induction motor control system. To do this, the speed observer is designed based on the combination of the sliding mode and the fractional order integral.

Design/methodology/approach – Super-twisting sliding mode (STSM) and Grünwald–Letnikov approach are used on the proposed observer. The stability of the proposed observer is verified by using Lyapunov method. Then, the observer coefficients are optimized for minimizing the steady-state error and chattering amplitude. The optimum coefficients (c_1, c_2, k_i and λ) are obtained by using response surface method. To verify the effectiveness of proposed observer, a large number of experiments are performed for different operation conditions, such as different speeds (500, 1,000 and 1,500 rpm) and loads (100 and 50 per cent loads). Parameter uncertainties (rotor inertia J and friction factor F) are tested to prove the robustness of the proposed method. All these operation conditions are applied for both proportional integral (PI) and fractional order STSM (FOSTSM) observers and their performances are compared.

Findings – The observer model is tested with optimum coefficients to validate the proposed observer effectiveness. At the beginning, the motor is started without load. When it reaches reference speed, the motor is loaded. Estimated speed and actual speed trends are compared. The results are presented in tables and figures. As a result, the FOSTSM observer has less steady-state error than the PI observer for all operation conditions. However, chattering amplitudes are lower in some operation conditions. In addition, the proposed observer shows more robustness against the parameter changes than the PI observer.

Practical implications – The proposed FOSTSM observer can be applied easily for industrial variable speed drive systems which are using induction motor to improve the performance and stability.

Originality/value – The robustness of the STSM and the memory-intensive structure of the fractional order integral are combined to form a robust and flexible observer. This paper grants the lower steady-state error and chattering amplitude for sensorless speed control of the induction motor in different speed and load operation conditions. In addition, the proposed observer shows high robustness against the parameter uncertainties.

Keywords Fractional calculus, Sliding mode control, Observers, Induction motors

Paper type Research paper

1. Introduction

To meet the need of reducing the cost of industrial systems, sensorless control applications on electrical machines are increasing day by day. In variable speed control systems, the

This study was supported by Scientific Research Projects Unit of Balikesir University (Project No: BAP. 2017/072).

COMPEL - The international journal for computation and mathematics in electrical and electronic engineering
Vol. 38 No. 2, 2019
pp. 878-892

0332-1649
DOI 10.1108/COMPEL-08-2018-0306

induction motors are more preferred to DC motors because of its low-cost, requiring less maintenance, robust construction and smaller size per kW output power. Although their many advantages, they also have disadvantages such as complex driver structures and controller algorithms (*Demirtas et al.*, 2018). The driver circuit is simply combined of six semiconductor switches (metal oxide semiconductor field effect transistor or insulated gate bipolar transistor). To generate gate signals, vector control or voltage/frequency (V/f) control methods are commonly used in industrial systems. Nowadays, the vector control method is more preferred for the gate controller algorithm to the V/f method because of its better performance at low speeds.

The most important way to reduce the cost of variable speed control systems is to get rid of the optic or magnetic-based position sensors. The angular velocity of the motor can be calculated without using a sensor. The mathematical model of the motor is used to achieve this. First of all, the mathematical model is established. Then, phase currents and voltages are obtained from current and voltage transducers which are quite cheap compared to the position sensors. The obtained current and voltage data are used in the model to estimate the motor position. This process is called model reference adaptive system (MRAS)-based position observer.

Many methods can be applied for motor position observer such as Luenberger (Orlowska-Kowalska, 1989; Kwon *et al.*, 2005), kalman filter (Bolognani *et al.*, 2003), sliding mode (Qiao *et al.*, 2013; Foo and Rahman, 2010; Benchaib *et al.*, 1999; Jiacai *et al.*, 2012), artificial neural network (Gadoue *et al.*, 2009; Hussain and Bazaz, 2016), fuzzy logic (Karanayil *et al.*, 2005; Gadoue *et al.*, 2010) and robust control (Mohamed, 2007; Yao *et al.*, 2014). There are many studies in the literature about observer, sliding mode control and fractional control used in electric motors. Di Gennaro *et al.* (2014) presented a sensorless control scheme for induction motor with core loss. In this study, two sensorless control schemes (high order sliding mode twisting algorithm and super-twisting sliding mode [STSM] algorithm) for induction motors have been designed. The proposed methods have been tested in simulations and experimental setup. As a result, both methods showed successful performance. Aurora and Ferrara (2007) proposed second order sliding mode speed and flux observer for induction motor. This method also has second-order super-twisting load torque estimator. They tested the performances and robustness of the proposed method by simulation and experimental results. Liu *et al.* (2014) presented a sliding mode observer for power factor control of AC/DC converter for hybrid electrical vehicles. They used STSM observer for estimating the input currents and load resistance. Simulation results show that the proposed observer-based controller has better performance compared to classical proportional integral (PI) control under disturbance effects and parametric uncertainty. Chang *et al.* (2011) proposed a fractional order integral sliding mode observer for induction motor. They used the Lyapunov method for design of the flux vector components (φ_d and φ_q). They tested the proposed method on digital signal processor (DSP)-/FPGA-based experimental setup. The results show that the proposed observer has better transient and steady state responses subject to load disturbances. Chi and Cheng (2014) presented the implementation of sensorless sliding mode drive for high-speed micro permanent magnet synchronous motor (PMSM). They used an electric dental hand piece motor and a 16-bit microcontroller. The authors expressed that the proposed sliding mode method is effective in motor applications in wide speed range. Hosseyni *et al.* (2015) presented a sliding mode observer for five phase PMSM. They designed the observer using the back electromotive force of PMSM. The proposed observer stability is verified by using the Lyapunov stability criteria. The results show that the proposed method offers satisfactory performance on load disturbance rejection and speed tracking. Wang *et al.* (2014) proposed a predictive torque control for induction machine. They used MRAS to estimate the rotor angular speed and stator-rotor fluxes. The experimental results show that the proposed method has fast dynamic structure. It has fine performance at steady state and transient state, and it can be used in wide speed range. Dadras and Momeni (2011) proposed a fractional order sliding mode observer for estimation of the fractional order system state variables. This study shows that the proposed observer can be applied on uncertain fractional order nonlinear systems. The proposed observer performance was presented with simulations. Urbański and Zawirski (2004) presented an adaptive observer for sensorless control of PMSM. They used a corrector in the model of the proposed observer and adjusted the corrector settings by using a proportional double integral type adaptation. The proposed observer was tested on DSP-based PMSM speed control system and they obtained successful results. *Holakooie et al.* (2018) presented a second-order sliding mode speed observer for a six-phase induction motor. The proposed observer is robust against DC-offsets and parameter uncertainties. Simulation and experimental results confirm the effectiveness of the proposed observer method. *Comanescu* (2016) presented a robust sliding mode observer for the flux magnitude of the induction motor. Proposed observer is compared with a similar flux observer. The results show that the proposed method is more robust to parameter variations.

Optimization of the performance of the industrial control systems is one of the most encountered problems nowadays. A lot of methods can be used for optimization such as artificial neural network (Zăvoianu *et al.*, 2013), genetic algorithm (Montazeri-Gh *et al.*, 2006), Ziegler–Nichols (Adhikari *et al.*, 2012), fuzzy logic (Ramesh *et al.*, 2006) and response surface method (RSM) (Ilten and Demirtas, 2016; Demirtas and Karaoglan, 2012; Jolly *et al.*, 2005). RSM is an easy applicable optimization method and more preferred in applications these days. This method can perform successful results by using only a few data.

This paper is organized as follows: in Section 2, dynamic model of induction motor is explained; in Section 3, fractional order integral expressions are given; STSM observer is given in Section 4; the simulation results are presented in Section 5; and finally, conclusion is given in Section 6.

2. Dynamic model of induction motor

Stationary *d-q* axis coordinate system model of the induction motor can be described as following (Rehman *et al.*, 2002):

$$\begin{bmatrix} \dot{i}_{ds} \\ \dot{i}_{qs} \end{bmatrix} = k_1\left(\begin{bmatrix} \eta & \omega_r \\ -\omega_r & \eta \end{bmatrix}\begin{bmatrix} f_{dr} \\ f_{qr} \end{bmatrix} - \eta L_m \begin{bmatrix} i_{ds} \\ i_{qs} \end{bmatrix}\right) - k_2\begin{bmatrix} i_{ds} \\ i_{qs} \end{bmatrix} + k_3\begin{bmatrix} v_{ds} \\ v_{qs} \end{bmatrix} \tag{1}$$

then the fluxes are:

$$\begin{bmatrix} \dot{\phi}_{dr} \\ \dot{\phi}_{qr} \end{bmatrix} = -\left(\begin{bmatrix} \eta & \omega_r \\ -\omega_r & \eta \end{bmatrix}\begin{bmatrix} \phi_{dr} \\ \phi_{qr} \end{bmatrix} - \eta L_m \begin{bmatrix} i_{ds} \\ i_{qs} \end{bmatrix}\right) \tag{2}$$

coefficients in equations (1) and (2) are:

$$k_1 = \frac{k_3 L_m}{L_r},\ k_2 = \frac{R_s}{\sigma L_s},\ k_3 = \frac{1}{\sigma L_s},\ \sigma = 1 - \frac{L_m^2}{L_s L_r},\ \eta = \frac{R_r}{L_r} \tag{3}$$

ϕ, V and I are the flux, voltage and current, respectively (subscripts r and s represent the rotor and stator). L_s and R_s are the stator inductance and resistance. L_m is the mutual inductance between the stator and rotor. ω_r is the rotor angular speed and σ is the flux leakage coefficient.

3. Fractional order integral

There are many definition types of fractional order derivative and integral. The definitions should be chosen for the structure of the problem (Petráš, 2011). The Grünwald–Letnikov definition is chosen in this study and can be defined as follows:

$$ {}_0D_t^{\alpha}x(t) = \lim_{h\to 0}\frac{1}{h^{\alpha}}\sum_{k=0}^{[t/h]}(-1)^k\binom{a}{k}x(t-kh) \tag{4}$$

$$ \binom{\alpha}{k} = \frac{\Gamma(\alpha+1)}{\Gamma(k+1)\Gamma(\alpha-k+1)} \tag{5}$$

where α is the derivative order ($n-1 \leq \alpha < n,\ n \in N^{+}$),$\Gamma$ is the gamma function of Euler, x is a time dependent function and h is a time increment. The order α can be changed with $-\lambda$, then the fractional order integral is defined as I^{λ}. If the limit operation is removed from equation (4), the fractional integral can be calculated by dividing the time interval [0,T] to N equal parts. Each parts has $h = 1/N$ sized. The nodes can be labeled as 0, 1, 2, 3,. . ., N, and I^{λ} at node M is obtained as following equation (Ilten and Demirtas, 2016; Ilten, 2013):

$$ {}_0I_t^{\lambda}x(t) = {}_0D_t^{-\lambda}x(hM) = \frac{1}{h^{-\lambda}}\sum_{j=0}^{M}w_j^{(-\lambda)}x(hM-jh) \tag{6}$$

$$ w_0^{(-\lambda)} = 1, \qquad w_j^{(-\lambda)} = \left(1-\frac{-\lambda+1}{j}\right)w_{j-1}^{(-\lambda)}, \quad j = 1,2,\ldots N \tag{7}$$

where w is the weight function and λ is the order of the integral.

4. Fractional order super-twisting sliding mode observer

The chattering effect in classical sliding mode is one of the biggest problems encountered. The chattering problem causes decreasing accuracy of the controllers, wearing of moving mechanical parts and overheating of the power circuits. This problem reduces the practical applicability of classical sliding mode. STSM, one of the high-order sliding mode methods, can be used to eliminate this problem. The basic STSM equation for manifold s can be described as follows (Rivera, 2011):

$$ \begin{aligned} u &= -\alpha_1\sqrt{|s|}sign(s) + v \\ \dot{v} &= -\alpha_2 sign(s) \end{aligned} \tag{8}$$

where u is the controller signal, α_1 and α_2 are the controller coefficients and *sign*() is the signum function. The design of the observer estimated current and flux equations are defined as:

$$ \begin{bmatrix} \dot{\hat{i}}_{ds} \\ \dot{\hat{i}}_{qs} \end{bmatrix} = k_1\left(\begin{bmatrix} \eta & \omega_r \\ -\omega_r & \eta \end{bmatrix}\begin{bmatrix} \hat{\phi}_{dr} \\ \hat{\phi}_{qr} \end{bmatrix} - \eta L_m\begin{bmatrix} \hat{i}_{ds} \\ \hat{i}_{qs} \end{bmatrix}\right) - k_2\begin{bmatrix} \hat{i}_{ds} \\ \hat{i}_{qs} \end{bmatrix} + k_3\begin{bmatrix} v_{ds} \\ v_{qs} \end{bmatrix} \tag{9}$$

$$\begin{bmatrix} \dot{\hat{\phi}}_{dr} \\ \dot{\hat{\phi}}_{qr} \end{bmatrix} = -\left(\begin{bmatrix} \eta & \omega_r \\ -\omega_r & \eta \end{bmatrix} \begin{bmatrix} \hat{\phi}_{dr} \\ \hat{\phi}_{qr} \end{bmatrix} - \eta L_m \begin{bmatrix} \hat{i}_{ds} \\ \hat{i}_{qs} \end{bmatrix} \right) \tag{10}$$

The current estimation errors are given below.

$$\begin{aligned} \tilde{i}_{ds} &= \hat{i}_{ds} - i_{ds} = e_d \\ \tilde{i}_{qs} &= \hat{i}_{qs} - i_{qs} = e_q \end{aligned} \tag{11}$$

and the sliding manifolds s_d and s_q can be described as:

$$s_d = \begin{cases} e_d & \text{for } |e_d| \leq e_d^0 \\ e_d^0 & \text{for } |e_d| > e_d^0 \end{cases} \tag{12}$$

$$s_q = \begin{cases} e_q & \text{for } |e_q| \leq e_q^0 \\ e_q^0 & \text{for } |e_q| > e_q^0 \end{cases} \tag{13}$$

Fractional order super-twisting sliding mode (FOSTSM) observer output for $d-q$ axis y can be defined as follows:

$$\begin{aligned} y_{d,q} &= -c_1\sqrt{|s_{d,q}|}sign(s_{d,q}) + v_{d,q} + I^\lambda s_{d,q} \\ \dot{v}_{d,q} &= -c_2 sign(s_{d,q}) \end{aligned} \tag{14}$$

where I^λ is the fractional integral in equation (6), c_1 and c_2 are the observer coefficients. $y_{d,q}$ expression means y_d and y_q axis outputs. The Lyapunov candidate function was used on equation (14) to prove that the system is stable. This equation is given below.

$$\begin{aligned} V_{d,q} &= 2c_2|s_{d,q}| + \frac{1}{2}v^2 + \frac{1}{2}\left(c_1\sqrt{|s_{d,q}|}sign(s_{d,q}) - v_{d,q}\right)^2 + |I^\lambda s_{d,q}| \\ &= \beta^T P \beta \end{aligned} \tag{15}$$

Where $\beta^T = \left(\sqrt{s_{d,q}}sign(s_{d,q})v\right)$ and $P = \frac{1}{2}\begin{pmatrix} 4c_2 + c_1^2 & -c_1 \\ -c_1 & 2 \end{pmatrix}$

The derivation of equation (15) is:

$$\dot{V}_{d,q} = -\frac{1}{|\sqrt{s_{d,q}}|}\beta^T Q \beta + \frac{s_{d,q}}{|\sqrt{s_{d,q}}|}\gamma^T \beta \tag{16}$$

where $Q = \frac{c_1}{2}\begin{pmatrix} 2c_2 + c_1^2 & -c_1 \\ -c_1 & 1 \end{pmatrix}$ and $\gamma^T = \left(2c_2 + \frac{1}{2}c_1^2 - \frac{1}{2}c_1\right)$. If we apply the bound for perturbations which is proposed by Moreno and Osorio (2008), the derivative of the Lyapunov function is reduced to following equation.

$$\dot{V}_{d,q} = -\frac{c_1}{2|\sqrt{s_{d,q}}|}\beta^T \tilde{Q} \beta \tag{17}$$

where $\tilde{Q} = \begin{pmatrix} 2c_2 + c_1^2 - \left(\frac{4c_2}{c_1} + c_1\right)\delta & -c_1 + 2\delta \\ -c_1 + 2\delta & 1 \end{pmatrix}$. If the controller gains satisfaction by these equations, the system is stable:

$$c_1 > 2\delta, \quad c_2 > c_1 \frac{5\delta c_1 + 4\delta^2}{2(c_1 - 2\delta)}, \quad \tilde{Q} > 0 \tag{18}$$

Estimated flux equations are given belows:

$$\begin{bmatrix} \dot{\hat{\phi}}_{dr} \\ \dot{\hat{\phi}}_{qr} \end{bmatrix} = \begin{bmatrix} \frac{1}{c_1 k_1} y_d - \frac{k_2}{k_1} \tilde{i}_{ds} + \frac{c_2}{c_1 k_1} I^{\lambda} \tilde{i}_{ds} \\ \frac{1}{c_1 k_1} y_q - \frac{k_2}{k_1} \tilde{i}_{qs} + \frac{c_2}{c_1 k_1} I^{\lambda} \tilde{i}_{qs} \end{bmatrix} \tag{19}$$

The induction motor speed can be derived from the equation (10). The estimated speed is:

$$\hat{\omega}_r = \frac{\hat{\phi}_{qr} \dot{\hat{\phi}}_{qr} - \dot{\hat{\phi}}_{qr} \hat{\phi}_{qr} - \eta L_m \left(\hat{i}_{qs} \hat{\phi}_{dr} - \hat{i}_{ds} \hat{\phi}_{qr} \right)}{\hat{\phi}_{dr} 2 + \hat{\phi}_{qr} 2} \tag{20}$$

Parameter	Value
Rated Voltage (line-line)	460 V
Stator Resistance (R_s)	0.01485 Ω
Stator Inductance (L_s)	0.0003027 H
Rotor Resistance (R_r)	0.009295 Ω
Rotor Inductance (L_r)	0.0003027 H
Mutual Inductance (L_m)	0.01046 H
Rotor Inertia (J)	3.1 kg.m2
Friction Factor (F)	0.08 N.m.s
Pole Pairs (p)	2

Table I.
Induction motor parameters

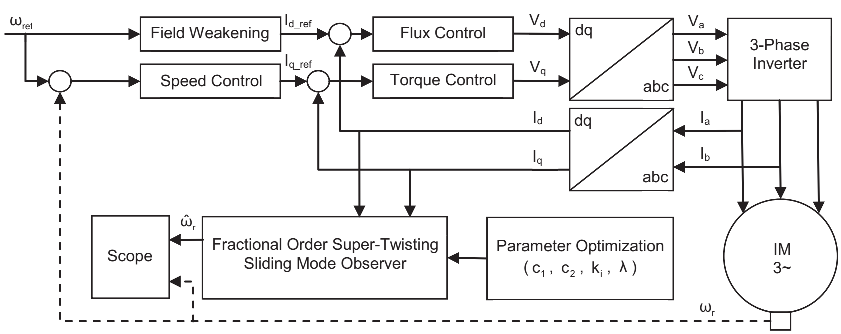

Figure 1.
Observer test block diagram for the induction motor speed control system

5. Simulation results

In this study, 150 kW squirrel cage induction motor is used. Motor parameters are listed in Table I. The proposed simulation model of the system is designed based on "AC3 - Sensorless Field-Oriented Control Induction Motor Drive" example of MATLAB/Simulink program (Motapon and Dessaint). In addition, the parameters in Table I are taken from this example. The proposed FOSTSM observer algorithm is written in a function block and used in the designed model. The estimated rotor speed which is the output of the observer block and the actual rotor speed are compared with using data on the scope. Observer test block diagram for the induction motor speed control system is shown in Figure 1.

In Figure 1, observer parameters c_1, c_2, k_i and λ are optimized by using RSM for minimizing the chattering effect and the steady-state error. General second-order polynomial RSM mathematical model is defined as below (Demirtas and Karaoglan, 2012):

$$Y_u = \beta_0 + \sum_{i=1}^{n} \beta_i X_{iu}^2 + \sum_{i<j}^{n} \beta_{ij} X_{iu} X_{ju} + e_u \tag{21}$$

Table II. RSM experiment table for FOSTSM observer

Experiment	c_1	c_2	k_i	λ	e_{ss}	cht
1	500	0.010	0.01	0.50	−1.280	0.045
2	3,000	0.010	0.01	0.50	0.150	0.750
3	500	20.000	0.01	0.50	−0.300	0.110
4	3,000	20.000	0.01	0.50	0.200	0.750
5	500	0.010	1,000.00	0.50	0.000	18.900
6	3,000	0.010	1,000.00	0.50	0.250	1.100
7	500	20.000	1,000.00	0.50	0.000	4.500
8	3,000	20.000	1,000.00	0.50	0.270	0.870
9	500	0.010	0.01	1.00	−0.280	0.050
10	3,000	0.010	0.01	1.00	0.150	0.710
11	500	20.000	0.01	1.00	−0.311	0.120
12	3,000	20.000	0.01	1.00	0.200	0.750
13	500	0.010	1,000.00	1.00	−0.290	0.080
14	3,000	0.010	1,000.00	1.00	0.150	0.720
15	500	20.000	1,000.00	1.00	−0.300	0.125
16	3,000	20.000	1,000.00	1.00	0.150	0.780
17	500	10.005	500.01	0.75	−0.742	0.160
18	3,000	10.005	500.01	0.75	0.170	0.710
19	1,750	0.010	500.01	0.75	0.100	0.500
20	1,750	20.000	500.01	0.75	0.150	0.650
21	1,750	10.005	0.01	0.75	0.150	0.610
22	1,750	10.005	1,000.00	0.75	0.150	0.550
23	1,750	10.005	500.01	0.50	0.150	1.000
24	1,750	10.005	500.01	1.00	0.150	0.590
25	1,750	10.005	500.01	0.75	0.150	0.560
26	1,750	10.005	500.01	0.75	0.150	0.560
27	1,750	10.005	500.01	0.75	0.150	0.560
28	1,750	10.005	500.01	0.75	0.150	0.560
29	1,750	10.005	500.01	0.75	0.150	0.560
30	1,750	10.005	500.01	0.75	0.150	0.560
31	1,750	10.005	500.01	0.75	0.150	0.560

In equation (21), Y_u is the system response; i and j are the linear and quadratic coefficients; β_0, β_i and β_{ij} are the regression coefficients; X_{iu} are coded values of ith input parameters and e_u is the residual experimental error of u_{th} observation.

Central composite full design is used for RSM, in this study. A total of 31 experiments are performed. The experimental results for FOSTSM observer are given in Table II.

In Table II, cht and e_{ss} are the chattering amplitude and the steady-state error, respectively. cht and e_{ss} based mathematical model of the system is given in equations (22) and (23).

$$\begin{aligned} cht = {} & 14.0 - 0.00418c_1 - 0.457c_2 + 0.01592k_i - 24.7\lambda + 0.000000c_1^2 + 0.0035c_2^2 \\ & + 0.000001k_i^2 + 9.1\lambda^2 + 0.000070c_1 * c_2 - 0.000002\, c_1 * k_i + 0.00453c_1 * \lambda \\ & - 0.000184c_2 * k_i + 0.370c_2 * \lambda - 0.01182k_i * \lambda \end{aligned} \tag{22}$$

Parameter	Value
c_1	1,410.6206
c_2	7.8842
k_i	222.8004
λ	0.8087

Table III. Optimal values of FOSTSM observer parameters

Experiment	k_p	k_i	e_{ss}	cht
1	5,000	5,000	−0.49	0.11
2	100,000	5,000	0.15	0.73
3	5,000	100,000	0.16	0.11
4	100,000	100,000	0.17	0.71
5	5,000	52,500	0.14	0.18
6	100,000	52,500	0.15	0.70
7	52,500	5,000	0.10	0.63
8	52,500	100,000	0.15	0.58
9	52,500	52,500	0.15	0.63
10	52,500	52,500	0.15	0.63
11	52,500	52,500	0.15	0.63
12	52,500	52,500	0.15	0.63
13	52,500	52,500	0.15	0.63

Table IV. RSM experiment table for PI observer

Parameter	Value
k_p	11,016.2323
k_i	49,676.4975

Table V. Optimal values of PI observer parameters

$$e_{ss} = -1.470 + 0.001269c_1 + 0.314c_2 + 0.000990k_i - 0.59\lambda - 0.000000c_1^2 + 0.00040c_2^2 + 0.000000k_i^2 + 1.04\lambda^2 - 0.000004c_1 * c_2 - 0.000000c_1 * k_i - 0.000124c_1 * \lambda - 0.000013c_2 * k_i - 0.0260c_2 * \lambda - 0.000900k_i * \lambda \quad (23)$$

The observer parameters c_1, c_2, k_i and λ are determined by using RSM to minimize the e_{ss} and *cht*. The optimal values of FOSTSM observer parameters are shown in Table III.

A comparison has been made to show the success of the proposed observer. To do this, classical PI type observer is used. PI observer is optimized under the same conditions as the proposed observer. The experimental results for PI observer are given in Table IV.

According to Table IV, *cht* and e_{ss}-based mathematical model of the system is given in equations (24) and (25).

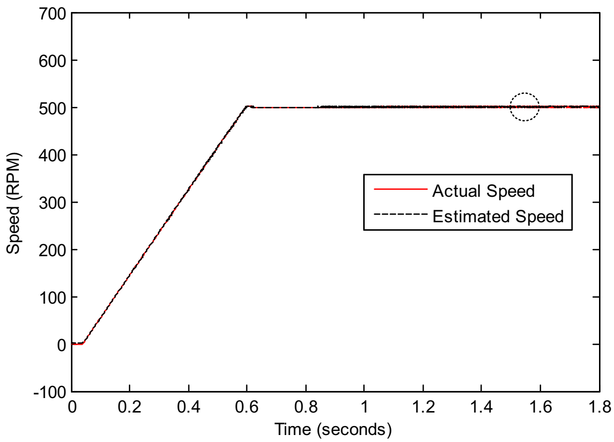

Figure 2.
The estimated and the actual speeds for PI observer

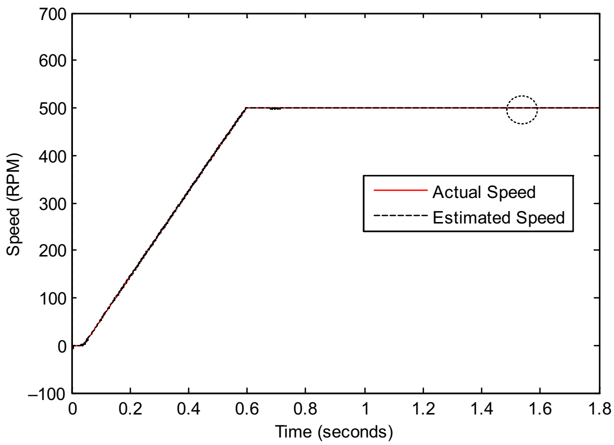

Figure 3.
The estimated and the actual speeds for FOSTSM observer

$$cht = 0.0536 + 0.00015k_p + 0.000001k_i - 0.000000k_p^2 - 0.000000k_i^2 - 0.000000k_p * k_i \quad (24)$$

$$ess = -0.461 + 0.000009k_p + 0.000010k_i - 0.000000k_p^2 - 0.000000k_i^2 - 0.000000k_p * k_i \quad (25)$$

PI observer parameters k_p and k_i are determined by using RSM to minimize the e_{ss} and *cht*. The optimal values of observer parameters are shown in Table V.

The observer models (PI and FOSTSM) are tested with these optimal values of parameters. The motor is started without load. It reaches 500 rpm reference speed at 0.6th s. At 0.7th s, the motor is fully loaded. Estimated speed and actual speed trends are compared in Figure 2 for PI observer and Figure 3 for FOSTSM observer. The zoomed graph of the steady state of the system (circled area in Figures 2 and 3) are shown in Figures 4 and 5.

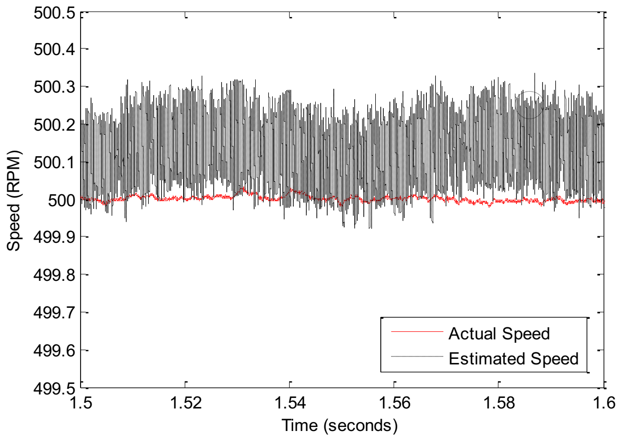

Figure 4.
The estimated and the actual speeds (zoomed graph) PI observer

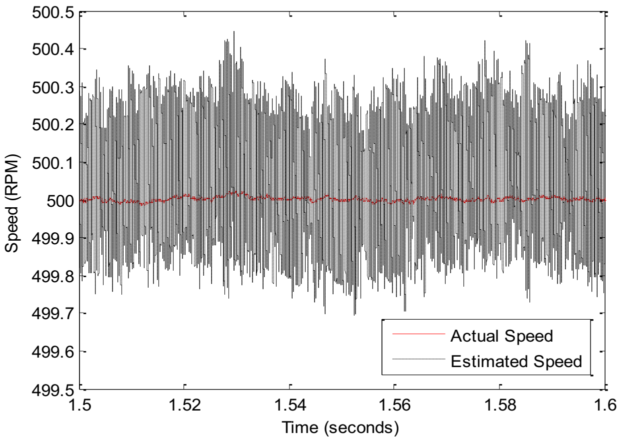

Figure 5.
The estimated and the actual speeds (zoomed graph) for FOSTSM observer

When Figures 2 and 4 are examined for PI observer, the e_{ss} and the *cht* values are 0.13 rpm (error is 0.026 per cent) and 0.22 rpm (error is 0.044 per cent), respectively. The e_{ss} and the *cht* values for FOSTSM observer are also examined on Figures 3 and 4. These values are obtained as 0.07 rpm (error is 0.014 per cent) and 0.42 rpm (error is 0.084 per cent). It is shown that the FOSTSM observer has less steady-state error but bigger chattering amplitude than the PI observer for this operation condition (500 rpm reference speed, 100 per cent load). In addition, both values are also less than 0.1 per cent. To verify the effectiveness of FOSTSM observer, a large number of experiments are performed for different operation conditions, such as different speeds (500, 1,000 and 1,500 rpm) and loads (100 and 50 per cent loads). Parameter uncertainties (rotor inertia J and friction factor F) are tested to prove the robustness of the proposed method. All these operation conditions are applied to the both of PI and FOSTSM observers and their performances are compared. The observers are also optimized for 1,000 and 1,500 rpm operation speeds for 100 and 50 per cent loads by using

Observer	Operation condition	Parameter	Value
PI	500 rpm, 100% load	k_p	11,016.2323
		k_i	49,676.4975
FOSTSM	500 rpm, 100% load	c_1	1,410.6206
		c_2	7.8842
		k_i	222.8004
		λ	0.8087
PI	500 rpm, 50% load	k_p	41,423.1824
		k_i	45,332.6475
FOSTSM	500 rpm, 50% load	c_1	1,818.3060
		c_2	4.5433
		k_i	782.3337
		λ	0.9549
PI	1000 rpm, 100% load	k_p	6,672.3823
		k_i	50,379.0519
FOSTSM	1000 rpm, 100% load	c_1	1,317.3953
		c_2	11.6435
		k_i	472.6829
		λ	0.7728
PI	1000 rpm, 50% load	k_p	39,685.6424
		k_i	29,154.9089
FOSTSM	1000 rpm, 50% load	c_1	1,044.1712
		c_2	14.1923
		k_i	928.0517
		λ	0.9545
PI	1500 rpm, 100% load	k_p	17,966.3923
		k_i	29,694.7874
FOSTSM	1500 rpm, 100% load	c_1	1,772.7687
		c_2	0.5380
		k_i	627.5083
		λ	0.7728
PI	1500 rpm, 50% load	k_p	16,228.8523
		k_i	24,482.1674
FOSTSM	1500 rpm, 50% load	c_1	2,273.5669
		c_2	0.0100
		k_i	113.8983
		λ	0.5000

Table VI.
Optimal values of observer parameters

Observer	Speed (rpm)	Load (%)	J (%)	F (%)	e_{ss} (rpm)	cht (rpm)	M_o (rpm)	M_u (rpm)	T_s (sec)
PI	500	100	100	100	0.13	0.22	0.55	−0.10	1.00
	500	100	80	100	0.16	0.27	0.55	−0.10	1.00
	500	100	120	100	0.15	0.23	0.55	−0.10	1.00
	500	100	100	80	0.15	0.25	0.55	−0.10	1.00
	500	100	100	120	0.15	0.24	0.55	−0.10	1.00
	500	50	100	100	0.07	0.57	1.40	−0.30	1.00
FOSTSM	500	100	100	100	0.07	0.42	0.55	−0.60	1.00
	500	100	80	100	0.07	0.42	0.55	−0.60	1.00
	500	100	120	100	0.07	0.42	0.55	−0.60	1.00
	500	100	100	80	0.07	0.42	0.55	−0.60	1.00
	500	100	100	120	0.07	0.42	0.55	−0.60	1.00
	500	50	100	100	0.01	0.52	1.40	−0.25	1.00
PI	1,000	100	100	100	0.35	0.30	2.10	0.15	1.50
	1,000	100	80	100	0.37	0.33	2.10	0.15	1.50
	1,000	100	120	100	0.36	0.34	2.10	0.15	1.50
	1,000	100	100	80	0.33	0.35	2.10	0.15	1.50
	1,000	100	100	120	0.33	0.38	2.10	0.15	1.50
	1,000	50	100	100	0.15	1.10	2.50	−0.40	1.50
FOSTSM	1,000	100	100	100	−0.05	0.50	1.90	−0.20	1.50
	1,000	100	80	100	−0.05	0.50	1.90	−0.20	1.50
	1,000	100	120	100	−0.05	0.50	1.90	−0.20	1.50
	1,000	100	100	80	−0.05	0.50	1.90	−0.20	1.50
	1,000	100	100	120	−0.05	0.50	1.90	−0.20	1.50
	1,000	50	100	100	0.02	0.37	1.90	−0.10	1.50
PI	1,500	100	100	100	1.44	1.13	2.50	−0.10	1.90
	1,500	100	80	100	1.45	1.10	2.50	−0.10	1.90
	1,500	100	120	100	1.43	1.15	2.50	−0.10	1.90
	1,500	100	100	80	1.42	1.17	2.50	−0.10	1.90
	1,500	100	100	120	1.38	1.05	2.50	−0.10	1.90
	1,500	50	100	100	1.40	1.20	2.40	−0.30	1.90
FOSTSM	1,500	100	100	100	0.65	0.76	2.10	−0.30	1.90
	1,500	100	80	100	0.65	0.76	2.10	−0.30	1.90
	1,500	100	120	100	0.65	0.76	2.10	−0.30	1.90
	1,500	100	100	80	0.65	0.76	2.10	−0.30	1.90
	1,500	100	100	120	0.65	0.76	2.10	−0.30	1.90
	1,500	50	100	100	0.68	2.15	2.50	−0.50	1.90

Table VII. Test results

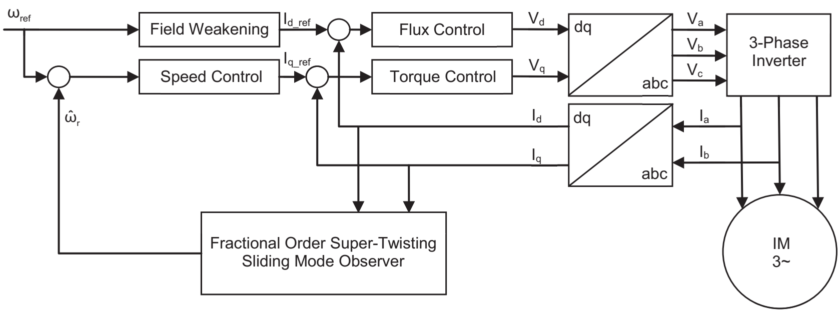

Figure 6. Sensorless block diagram of the speed control of the induction motor

RSM. The optimal values of observer parameters are given in Table VI and all test results are presented in Table VII.

In Table VII, M_o is the maximum overshoot, M_u is the maximum undershoot and T_s is the settling time. The values in Table VII show that the FOSTSM observer performance is unaffected from the parameter changes (J and F). As a result, the FOSTSM observer has less steady-state error than the PI observer for all operation conditions. However, chattering amplitudes are lower in some operation conditions. In addition, the proposed observer shows more robustness against the parameter changes than the PI observer.

After the optimization of the values of observer parameters, the speed sensor shown as dotted line in Figure 1 is removed from the block diagram. Sensorless block diagram of the speed control of the induction motor is presented in Figure 6.

6. Conclusion

In this study, FOSTSM observer is designed based on MRAS method for induction motor speed control system. Grünwald–Letnikov discrete fractional integral definition is used in STSM controller's integral part. The observer coefficients are optimized for minimizing the *cht* and the e_{ss}. The optimum coefficients (c_1, c_2, k_i and λ) are obtained by using RSM.

The designed observer has been compared with classical PI type observer to prove the success of it. A large number of experiments are performed for different operation conditions, such as different speeds (500, 1,000 and 1,500 rpm) and loads (100 and 50 per cent loads). Parameter uncertainties (rotor inertia J and friction factor F) are tested to prove the robustness of the proposed method. All these operation conditions are applied for both PI and FOSTSM observers and then their performances are compared with each other.

The simulation results show that the FOSTSM observer performance is unaffected from the parameter changes (J and F). As a result, the FOSTSM observer has less steady-state error than the PI observer for all operation conditions. However, chattering amplitudes are lower in some operation conditions. In addition, the proposed observer shows more robustness against the parameter changes than the PI observer. Therefore, the FOSTSM observer is more suitable to achieve high success in systems where e_{ss} accuracy is very important. Its robust structure makes the system more stable. This method can be applied effectively in solution of the fault detection problem of various applications of electrical machines, such as double-fed induction generator and synchronous generator.

References

Adhikari, N.P., Choubey, M., and Singh, R. (2012), "DC motor control using Ziegler Nichols and genetic algorithm technique", *International Journal of Electrical, Electronics and Computer Engineering*, Vol. 1, pp. 33-36.

Aurora, C. and Ferrara, A. (2007), "A sliding mode observer for sensorless induction motor speed regulation", *International Journal of Systems Science*, Vol. 38 No. 11, pp. 913-929.

Benchaib, A., Rachid, A., Audrezet, E. and Tadjine, M. (1999), "Real-time sliding-mode observer and control of an induction motor", *IEEE Transactions on Industrial Electronics*, Vol. 46 No. 1, pp. 128-138.

Bolognani, S., Tubiana, L. and Zigliotto, M. (2003), "Extended kalman filter tuning in sensorless PMSM drives", *IEEE Transactions on Industry Applications*, Vol. 39 No. 6, pp. 1741-1747.

Chang, Y.H., Wu, C.I., Chen, H.C., Chang, C.W. and Lin, H.W. (2011),"Fractional-order integral sliding-mode flux observer for sensorless vector-controlled induction motors", *American Control Conference (ACC), 2011. IEEE.*

Chi, W.-C. and Cheng, M.-Y. (2014), "Implementation of a sliding-mode-based position sensorless drive for high-speed micro permanent-magnet synchronous motors", *ISA Transactions*, Vol. 53 No. 2, pp. 444-453.

Comanescu, M. (2016), "Design and implementation of a highly robust sensorless sliding mode observer for the flux magnitude of the induction motor", *IEEE Transactions on Energy Conversion*, Vol. 31 No. 2, pp. 649-657.

Dadras, S. and Momeni, H.R. (2011), "Fractional sliding mode observer design for a class of uncertain fractional order nonlinear systems", *Decision and control and European control conference (CDC-ECC), 50th IEEE conference on, IEEE, 2011*.

Demirtas, M., Ilten, E. and Calgan, H. (2018), "Pareto-based multi-objective optimization for fractional order PI^{λ} speed control of induction motor by using Elman neural network", *Arabian Journal for Science and Engineering*, pp. 1-11, available at: https://doi.org/10.1007/s13369-018-3364-2

Demirtas, M. and Karaoglan, A.D. (2012), "Optimization of PI parameters for DSP-based permanent magnet brushless motor drive using response surface methodology", *Energy Conversion and Management*, Vol. 56, pp. 104-111.

Di Gennaro, S., Dominguez, J.R. and Meza, M.A. (2014), "Sensorless high order sliding mode control of induction motors with core loss", *IEEE Transactions on Industrial Electronics*, Vol. 61 No. 6, pp. 2678-2689.

Foo, G. and Rahman, M.F. (2010), "Sensorless sliding-mode MTPA control of an IPM synchronous motor drive using a sliding-mode observer and HF signal injection", *IEEE Transactions on Industrial Electronics*, Vol. 57 No. 4, pp. 1270-1278.

Gadoue, S.M., Giaouris, D. and Finch, J.W. (2009), "Sensorless control of induction motor drives at very low and zero speeds using neural network flux observers", *IEEE Transactions on Industrial Electronics*, Vol. 56 No. 8, pp. 3029-3039.

Gadoue, S.M., Giaouris, D. and Finch, J.W. (2010), "MRAS sensorless vector control of an induction motor using new sliding-mode and fuzzy-logic adaptation mechanisms", *IEEE Transactions on Energy Conversion*, Vol. 25 No. 2, pp. 394-402.

Holakooie, M.H., Ojaghi, M. and Taheri, A. (2018), "Modified DTC of Six-Phase induction motor with a second-order sliding-mode MRAS-based speed stimulator", *IEEE Transactions on Power Electronics*.

Hosseyni, A., Trabelsi, R., Mimouni, M.F., Iqbal, A. and Alammari, R. (2015), "Sensorless sliding mode observer for a five-phase permanent magnet synchronous motor drive", *ISA Transactions*, Vol. 58, pp. 462-473.

Hussain, S. and Bazaz, M.A. (2016), "Neural network observer design for sensorless control of induction motor drive", *IFAC-PapersOnLine*, Vol. 49 No. 1, pp. 106-111.

Ilten, E. and Demirtas, M. (2016), "Off-Line tuning of fractional order PIλ controller by using response surface method for induction motor speed control", *Journal of Control Engineering and Applied Informatics*, Vol. 18, pp. 20-27.

Ilten, E. (2013), "Asenkron motorun dsPIC tabanlı kesirli PI hız kontrolü", M.S. thesis, Institute of Science, Balikesir University, Balikesir, Turkey.

Jiacai, H., Hongsheng, L., Qinghong, X. and Di, L. (2012), "Sensorless vector control of PMSM using sliding mode observer and fractional-order phase-locked loop" *Control Conference (CCC), 2012 31st Chinese*, IEEE.

Jolly, J., Jabbar, M.A. and Qinghua, L. (2005), "Design optimization of permanent magnet motors using response surface methodology and genetic algorithms", *IEEE Transactions on Magnetics*, Vol. 41 No. 10, pp. 3928-3930.

Karanayil, B., Rahman, M.F. and Grantham, C. (2005), "Stator and rotor resistance observers for induction motor drive using fuzzy logic and artificial neural networks", *IEEE Transactions on Energy Conversion*, Vol. 20 No. 4, pp. 771-780.

Kwon, T.-S., Shin, M.-H. and Hyun, D.-S. (2005), "Speed sensorless stator flux-oriented control of induction motor in the field weakening region using Luenberger observer", *IEEE Transactions on Power Electronics*, Vol. 20 No. 4, pp. 864-869.

Liu, J., Laghrouche, S. and Wack, M. (2014), "Observer-based higher order sliding mode control of power factor in three-phase AC/DC converter for hybrid electric vehicle applications", *International Journal of Control*, Vol. 87 No. 6, pp. 1117-1130.

Mohamed, Y.A.-R.I. (2007), "Design and implementation of a robust current-control scheme for a PMSM vector drive with a simple adaptive disturbance observer", *IEEE Transactions on Industrial Electronics*, Vol. 54 No. 4, pp. 1981-1988.

Montazeri-Gh, M., Poursamad, A. and Ghalichi, B. (2006), "Application of genetic algorithm for optimization of control strategy in parallel hybrid electric vehicles", *Journal of the Franklin Institute*, Vol. 343 Nos 4/5, pp. 420-435.

Moreno, J.A. and Osorio, M. (2008), "A Lyapunov approach to second-order sliding mode controllers and observers", *Decision and Control, 2008. CDC 2008. 47th IEEE Conference on, IEEE.*

Orlowska-Kowalska, T. (1989), "Application of extended Luenberger observer for flux and rotor time-constant estimation in induction motor drives", *IEE Proceedings D (Control Theory and Applications)*, IET Digital Library, Vol. 136 No. 6.

Petráš, I. (2011), *Fractional-Order Nonlinear Systems: modeling, Analysis and Simulation*, Springer Science and Business Media.

Qiao, Z., Shi, T., Wang, Y., Yan, Y., Xia, C. and He, X. (2013), "New sliding-mode observer for position sensorless control of permanent-magnet synchronous motor", *IEEE Transactions on Industrial Electronics*, Vol. 60 No. 2, pp. 710-719.

Ramesh, L., Chowdhury, S.P., Chowdhury, S., Saha, A.K. and Song, Y.H. (2006), "Efficiency optimization of induction motor using a fuzzy logic based optimum flux search controller" *Power Electronics, Drives and Energy Systems, PEDES'06. International Conference on, IEEE.*

Rehman, H.U., Derdiyok, A., Guven, M.K. and Xu, L. (2002), "A new current model flux observer for wide speed range sensorless control of an induction machine", *IEEE Transactions on Power Electronics*, Vol. 17 No. 6, pp. 1041-1048.

Rivera, J., Garcia, L., Mora, C., Raygoza, J.J. and Ortega, S. (2011), "Super-twisting sliding mode in motion control systems", *Sliding Mode Control*, InTech.

Urbański, K. and Zawirski, K. (2004), "Adaptive observer of rotor speed and position for PMSM sensorless control system", *Compel - the International Journal for Computation and Mathematics in Electrical and Electronic Engineering*, Vol. 23 No. 4, pp. 1129-1145.

Wang, F., Chen, Z., Stolze, P., Stumper, J.F., Rodríguez, J. and Kennel, R. (2014), "Encoderless finite-state predictive torque control for induction machine with a compensated MRAS", *IEEE Transactions on Industrial Informatics*, Vol. 10 No. 2, pp. 1097-1106.

Yao, J., Jiao, Z. and Ma, D. (2014), "Adaptive robust control of DC motors with extended state observer", *IEEE Transactions on Industrial Electronics*, Vol. 61 No. 7, pp. 3630-3637.

Zăvoianu, A.C., Bramerdorfer, G., Lughofer, E., Silber, S., Amrhein, W. and Klement, E.P. (2013), "Hybridization of multi-objective evolutionary algorithms and artificial neural networks for optimizing the performance of electrical drives", *Engineering Applications of Artificial Intelligence*, Vol. 26 No. 8, pp. 1781-1794.

Further reading

Souleman, N.M. and Louis-A, D. "AC3 – Sensorless field-oriented control induction modtor rive", MATLAB/Simulink example.

Corresponding author

Erdem Ilten can be contacted at: erdemilten@balikesir.edu.tr